JCB Article

Steady-state dynamics of Cajal body components in the *Xenopus* germinal vesicle

Korie E. Handwerger,[1,2] Christine Murphy,[1] and Joseph G. Gall[1]

[1]Department of Embryology, Carnegie Institution of Washington, Baltimore, MD 21210
[2]Department of Biology, Johns Hopkins University, Baltimore, MD 21218

Cajal bodies (CBs) are evolutionarily conserved nuclear organelles that contain many factors involved in the transcription and processing of RNA. It has been suggested that macromolecular complexes preassemble or undergo maturation within CBs before they function elsewhere in the nucleus. Most such models of CB function predict a continuous flow of molecules between CBs and the nucleoplasm, but there are few data that directly support this view. We used fluorescence recovery after photobleaching (FRAP) on isolated *Xenopus* oocyte nuclei to measure the steady-state exchange rate between the nucleoplasm and CBs of three fluorescently tagged molecules: U7 small nuclear RNA, coilin, and TATA-binding protein (TBP). In the nucleoplasm, the apparent diffusion coefficients for the three molecules ranged from 0.26 to 0.40 $\mu m^2\ s^{-1}$. However, in CBs, fluorescence recovery was markedly slower than in the nucleoplasm, and there were at least three kinetic components. The recovery rate within CBs was independent of bleach spot diameter and could not be attributed to high CB viscosity or density. We propose that binding to other molecules and possibly assembly into larger complexes are the rate-limiting steps for FRAP of U7, coilin, and TBP inside CBs.

Introduction

Cajal bodies (CBs)* were first described almost a century ago (Cajal, 1903), but their molecular characterization did not begin until the 1990s, when it was discovered that they were specifically stained by human autoantibodies. One such antibody recognized a novel protein of unknown function, p80-coilin, which has been used extensively as a marker protein for CBs (Andrade et al., 1991; Raška et al., 1991). A plethora of other proteins and RNAs were subsequently identified as CB constituents. These included RNA polymerase I, II, and III subunits, basal transcription factors, and RNA processing factors such as snRNPs (for review see Matera, 1999; Gall, 2000). Importantly, CBs do not contain nascent RNA or hnRNPs. Thus, it is unlikely that CBs are sites of transcription, splicing, or storage of partially processed RNAs that are bound for the cytoplasm. Alternatively, they may function in maturation and/or preassembly of transcription and processing complexes before their distribution to other parts of the nucleus.

Targeting of epitope-tagged molecules to CBs provides evidence that some components may transit through CBs on their way to sites of transcription in the nucleus (Gall et al., 1999; Narayanan et al., 1999; Gall, 2000). Similarly, in vivo visualization of CB components tagged with GFP suggests that some molecules localize to CBs as a primary step in RNP maturation (Sleeman et al., 1998; Sleeman and Lamond, 1999; Verheggen et al., 2001, 2002). Such studies imply that CBs play an active role in RNA biogenesis, but leave open the question of how individual CB components behave at steady state.

The application of photophysical techniques to live-cell imaging has transformed our understanding of nuclear dynamics. In particular, FRAP and related techniques (Axelrod et al., 1976; Dewey, 1991) have made it clear that many proteins rapidly and continuously enter and exit nuclear organelles, even though their steady-state distributions give the impression that they might be stable components of these organelles (Misteli et al., 1997; Phair and Misteli, 2000, 2001; Snaar et al., 2000; Chen et al., 2002; Dundr et al., 2002).

In this work, we extend the analysis of CB structure and function by observing the steady-state behavior of three

The online version of this article includes supplemental material.

Address correspondence to Joseph G. Gall, Dept. of Embryology, Carnegie Institution of Washington, 115 West University Parkway, Baltimore, MD 21210. Tel.: (410) 554-1217. Fax: (410) 243-6311. E-mail: gall@ciwemb.edu

K.E. Handwerger's present address is Whitehead Institute for Biomedical Research, Nine Cambridge Center, Cambridge, MA 02142.

*Abbreviations used in this paper: CB, Cajal body; GV, germinal vesicle; snRNA, small nuclear RNA; TBP, TATA-binding protein; TMG, trimethylguanosine.

Key words: coilin; diffusion; FRAP; TATA-binding protein; U7 snRNA

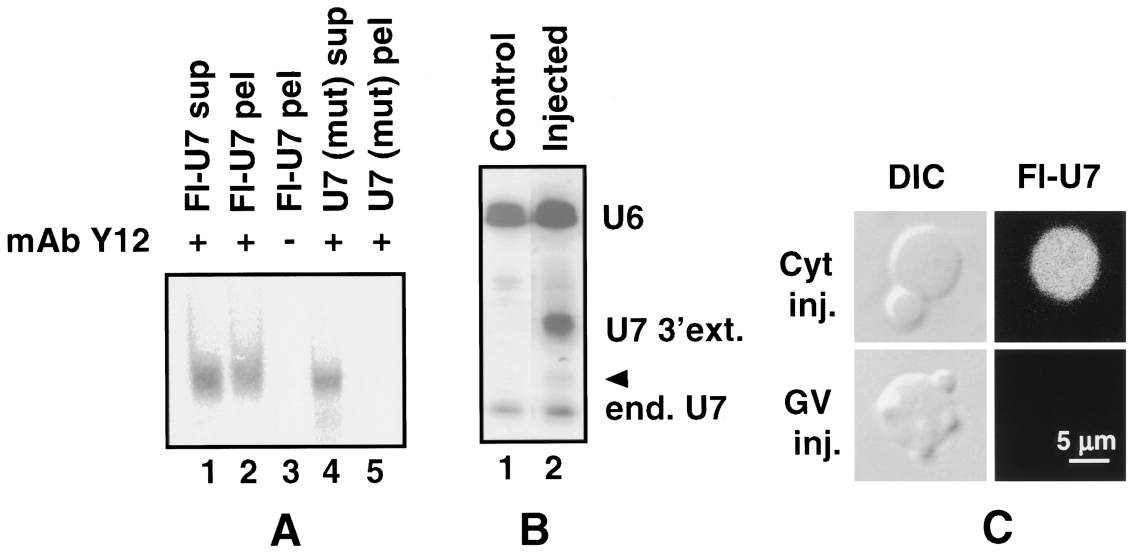

Figure 1. **When injected into the cytoplasm, fluorescein-U7 snRNA is assembled into a stable snRNP complex that is targeted to the nucleoplasm and to CBs.** (A) Autoradiograph of ^{32}P-labeled snRNAs that were injected into the cytoplasm, recovered the next day from oocyte extract, and immunoprecipitated with anti-Sm mAb Y12. Fluorescein-U7 is immunoprecipitated (lane 2), whereas fluorescein-U7 that contains a mutant Sm-binding site is not (lane 5). Control beads without antibody do not precipitate fluorescein-U7 (lane 3). Pel, material recovered from washed beads; Sup, 10% of supernatant after incubation with beads. (B) Northern blot comparing the total amount of endogenous and injected U7 snRNA in whole GVs. Lane 1, endogenous U7 (end. U7) from 3 control GVs; lane 2, Endogenous and injected U7 (U7 3′ ext.) from 3 GVs isolated 8 h after cytoplasmic injection. Endogenous U6 snRNA serves as a loading control. Arrowhead points to minor breakdown porduct. (C) Top panels; differential interference contrast and fluorescence images of a single brightly fluorescent CB in an oil-isolated GV, 18 h after cytoplasmic injection of fluorescein-U7. Bottom panels; an almost unlabeled CB in a GV that was removed under oil, injected with fluorescein-U7, and held overnight before observation.

fluorescently labeled CB components: U7 small nuclear RNA (snRNA), coilin, and TATA-binding protein (TBP). First, we demonstrate that exchange of CB components between the nucleoplasm and CBs is slow compared with their mobility in the nucleoplasm. Second, we find that the rate of fluorescence recovery in CBs is independent of the bleach spot diameter and is multi-phasic. Finally, we show that CBs are not appreciably more viscous or dense than the surrounding nucleoplasm. These data allow us to rule out diffusion as the rate-limiting factor in the movement of these three components in and out of CBs. Computer analyses of our FRAP data are most consistent with models in which each molecule exists in three distinct kinetic states within CBs. We conclude that CBs maintain their steady-state concentration of specific factors by selective, multi-state binding.

Results

Fluorescein-U7 snRNA, GFP-coilin, and GFP-TBP behave like endogenous U7 snRNA, coilin, and TBP

Before studying the trafficking of fluorescently tagged molecules, we compared several aspects of their behavior with that of the endogenous counterparts. We showed that fluorescein-U7 snRNA forms an Sm-snRNP, which is stable in the oocyte nucleus (germinal vesicle, or GV) and is properly localized to the nucleoplasm and CBs. The behavior of GFP-coilin was assessed by its stability in the GV and its targeting to CBs. For GFP-TBP, we confirmed that it targeted to the same nuclear structures that contain endogenous TBP, and that its overexpression did not inhibit transcription.

The U7 snRNP is involved in the maturation of histone pre-mRNAs. After being transcribed and exported to the cytoplasm, U7 snRNA receives a trimethylguanosine (TMG) cap and forms a complex with Sm- and snRNP-specific proteins before it is reimported into the nucleus (Birnstiel and Schaufele, 1988; Mattaj, 1988; Smith et al., 1991; Pillai et al., 2001). In the *Xenopus* GV, endogenous U7 snRNA is localized primarily in the CBs (Wu and Gall, 1993; Wu et al., 1996). Here, we show that fluorescein-U7 that has been injected into the oocyte cytoplasm, like endogenous U7, can be immunoprecipitated from GV extracts by mAb Y12 (Fig. 1 A). Y12 recognizes a symmetrical dimethylarginine epitope found on several Sm proteins and on coilin (Brahms et al., 2001; Hebert et al., 2002). Fluorescein-U7 that has been recovered from injected oocytes migrates at the expected molecular weight on a Northern blot, and shows little sign of degradation after prolonged incubation inside cells (Fig. 1 B). Finally, when fluorescein-U7 snRNA is injected into the oocyte cytoplasm, and GVs are subsequently isolated for cytological analysis, one sees brightly fluorescent CBs against a low level of nucleoplasmic staining (Fig. 1 C). In contrast, when fluorescein-U7 is injected directly into oil-isolated GVs, fluorescence is barely detectable in CBs, even after overnight incubation (Fig. 1 C). These results suggest that under standard conditions of cytoplasmic injection, fluorescein-U7 transcripts associate properly with Sm proteins in the cytoplasm before they enter the nucleus, where they are stable. Fluorescein-U7 snRNPs are then concentrated in CBs in a pattern that is indistinguishable from that of the endogenous snRNP.

Coilin was originally identified on the basis of autoimmune sera that specifically stained CBs (then called coiled

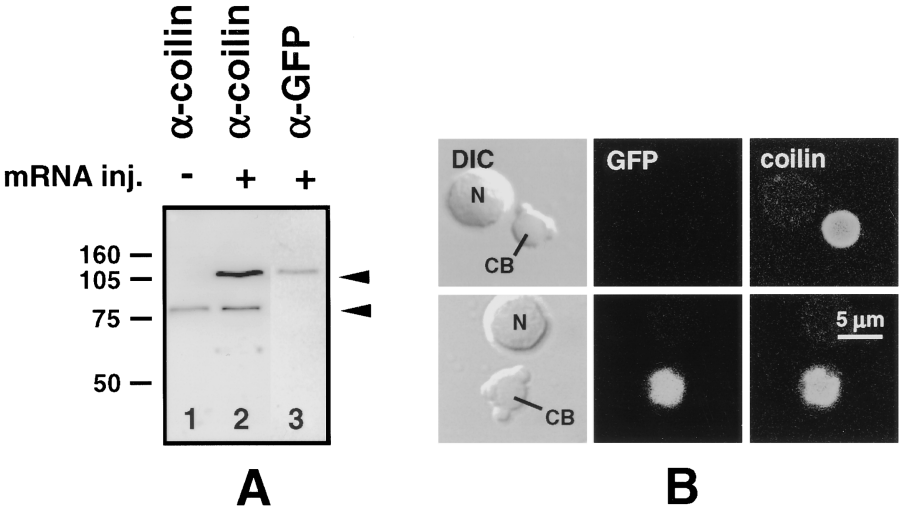

Figure 2. ***Xenopus* GFP-coilin is efficiently translated by *Xenopus* oocytes and is targeted to CBs.** (A) Western blot of GV proteins from control oocytes (lane 1) or oocytes injected with *Xenopus* GFP-coilin mRNA (lanes 2 and 3), stained with an antibody against *Xenopus* coilin (lanes 1 and 2) or against GFP (lane 3). The bottom band is endogenous coilin, the top band is newly translated GFP-coilin. Molecular mass standards in kD. (B) Confocal images of a CB from a control GV (top panels) and from a GV isolated from an oocyte that had been injected with GFP-coilin mRNA (bottom panels), stained with antibodies against GFP (middle panels) or coilin (right panels). In the injected oocyte, GFP-coilin and endogenous coilin are precisely colocalized. CB, Cajal body; N, nucleolus.

bodies; Andrade et al., 1991; Raška et al., 1991). Earlier studies suggested that coilin might be involved in the transport of snRNPs from the cytoplasm to CBs (Bauer and Gall, 1997; Bellini and Gall, 1998). This view is now strongly supported by evidence from coilin knockout mice (Tucker et al., 2001) and biochemical data showing an association between coilin and SMN, the spinal muscular atrophy gene (Hebert et al., 2001, 2002). In our experiments, in vitro-transcribed *Xenopus* GFP-coilin mRNA was efficiently translated when injected into the oocyte cytoplasm. The fusion protein, isolated from injected cells after overnight incubation, migrated at the anticipated molecular weight on Western blots and reacted with antibodies against both *Xenopus* coilin and GFP (Fig. 2 A). Consistent with previous observations (Wu et al., 1994; Handwerger et al., 2002), the fusion protein is readily targeted to CBs, as shown by the appearance of fluorescent CBs within several hours after injection of the mRNA (Fig. 2 B). These data indicate that the fusion protein is stable in the GV over the time course of our experiments, and that GFP does not disrupt the targeting of coilin to CBs.

Human GFP-TBP mRNA was also robustly translated by *Xenopus* oocytes. The fusion protein migrated at the anticipated molecular weight on Western blots, and was recognized by antibodies against GFP and human TBP (Fig. 3 A). Although the anti-TBP antibody did not react convincingly with endogenous *Xenopus* TBP on Western blots, it stained CBs more brightly than other structures in control GV spread preparations (Fig. 3 B). In spreads of GVs from injected oocytes, GFP fluorescence was also detected primarily in CBs (Fig. 3 B). Finally, the axes and lateral loops of the lampbrush chromosomes appeared fully extended in GV spreads from both control and injected cells (unpublished data), suggesting that RNA polymerase II transcription was not inhibited by overexpression of TBP.

Diffusion of fluorescein-U7, GFP-coilin, and GFP-TBP in the GV nucleoplasm

To study the kinetics of molecules in the nucleoplasm, we developed a high resolution method for observing the real-time behavior of CB components in oil-isolated GVs. In brief, fluorescein-U7, GFP-coilin mRNA, or GFP-TBP mRNA was

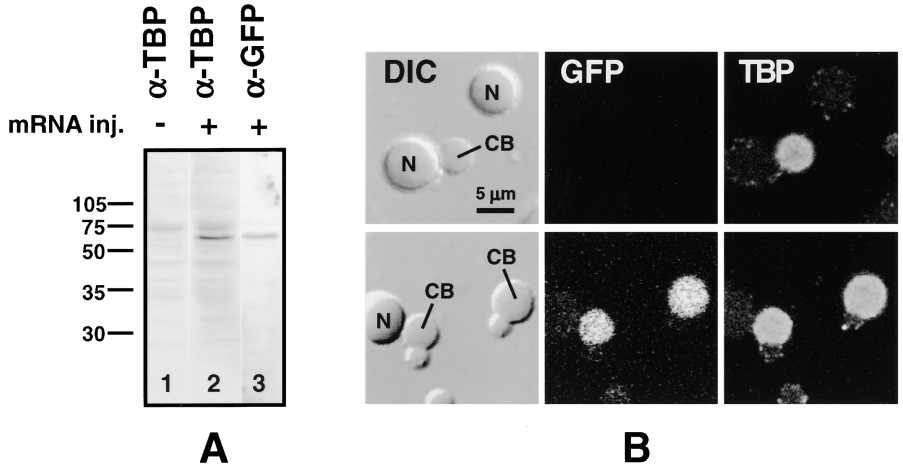

Figure 3. **Human GFP-TBP is efficiently translated by *Xenopus* oocytes and is targeted to CBs.** (A) Western blot of GV proteins from control oocytes (lane 1) or oocytes injected with human GFP-TBP mRNA (lanes 2 and 3), stained with an antibody against human TBP (lanes 1 and 2) or against GFP (lane 3). Both antibodies recognize a band of human GFP-TBP at ~60 kD. The weak band at ~40 kD in lanes 1 and 2 may represent endogenous TBP. (B) Confocal images of CBs from a control GV (top panels) and from a GV isolated from an oocyte that had been injected with human GFP-TBP mRNA (bottom panels), stained with antibodies against GFP (middle panels) or human TBP (right panels). In the injected oocyte, GFP-TBP and endogenous TBP are precisely colocalized. CB, Cajal body; N, nucleolus.

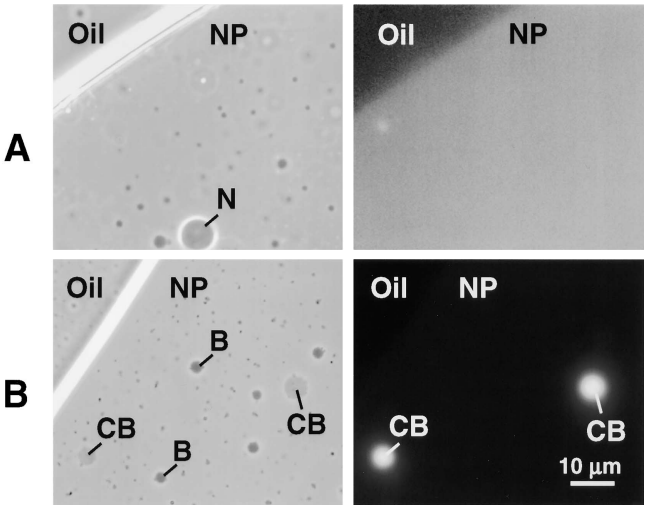

Figure 4. **Oil-isolated GV.** (A) Phase contrast (left) and fluorescence image (right) of part of an oil-isolated GV from an oocyte that had been injected with fluorescein-U7. A long exposure (10 s) taken at the oil–GV interface to show the diffuse pool of fluorescein-U7 in the nucleoplasm. (B) Similar images in a region of the GV that contains two CBs. In this short exposure (1 s), the brightly labeled CBs are conspicuous, but the weaker nucleoplasmic label is not evident. B, B-snurposome; CB, Cajal body; NP, nucleoplasm; N, nucleolus.

injected into the oocyte cytoplasm. After oocytes had incubated overnight at 18°C, GVs were removed in oil and gently squashed under a coverslip on a microscope slide. Unlike fixed GV preparations, in which the nuclear envelope is removed and the nucleoplasm is washed away during centrifugation, oil-isolated GVs preserve fluorescent molecules in the nucleoplasm as a potential pool for molecular exchange with CBs. In these preparations, CBs appear as bright fluorescent spheres in a background of diffusely fluorescent nucleoplasm (Fig. 4, A and B). To quantify the mobility of CB components in the nucleoplasm, we used a fluorescence microscope outfitted with custom hardware and software to measure FRAP on a millisecond time scale. Fig. 5 A shows a typical recovery curve for GFP-coilin in the nucleoplasm. In this example, fluorescence recovered rapidly over the first 3 s of the experiment, and then reached a plateau that was maintained for the duration of the experiment. Fig. 5 B summarizes the results of nucleoplasmic FRAP experiments with fluorescein-U7, GFP-coilin, and GFP-TBP. The apparent diffusion coefficients for these molecules in the nucleoplasm were 0.26 ± 0.08, 0.40 ± 0.14, and 0.33 ± 0.12 $\mu m^2 s^{-1}$, respectively, assuming a single diffusing component (Axelrod et al., 1976). These values are not significantly different from one another, and are similar to apparent diffusion coefficients for mRNA and nuclear proteins in the nucleoplasm of somatic cells (Politz et al., 1999; Phair and Misteli, 2000).

The concentration of U7 snRNP in CBs is invariant

We know that the final concentration of U7 snRNA and coilin (and presumably TBP) is higher in the nucleoplasm of injected oocytes than in controls (see Fig. 1 B, Fig. 2 A, and Fig. 7). Before measuring steady-state kinetics by FRAP, we compared the concentration of U7 snRNA in CBs of control and injected oocytes. We used mAb K121, an antibody that recognizes the TMG cap found on most mature snRNAs. It was previously shown that ~90% of K121 staining in the CB is due to U7 (Bellini and Gall, 1998). If CBs are saturable with respect to U7, the concentration of TMG and hence, of K121 staining should not increase when excess U7 is introduced into the GV. On the other hand, if CBs can incorporate exogenous U7 without growth or release of endogenous U7, K121 staining should increase. To determine TMG concentration, we plotted the total K121 fluorescence of individual CBs against their volume (Fig. 6). The data for CBs from control and injected oocytes are essentially superimposable. Both exhibit a linear relationship between fluorescence and CB volume, the slope of which is a measure of TMG concentration. These results demonstrate that although nucleoplasmic levels of U7 continue to rise due to continuous import from the cytoplasm, the concentration in CBs remains the same. These measurements suggest one of two possibilities (or a combination of the two). Either exogenous U7 displaces endogenous U7 in the CBs, implying an active flux of U7 through CBs, or CBs increase in volume without a change in U7 concentration, implying a more passive role for CBs, such as storage.

Exogenous U7 displaces endogenous U7 from CBs

To distinguish active flux from storage of U7 in CBs, we followed the distribution of exogenous and endogenous

A

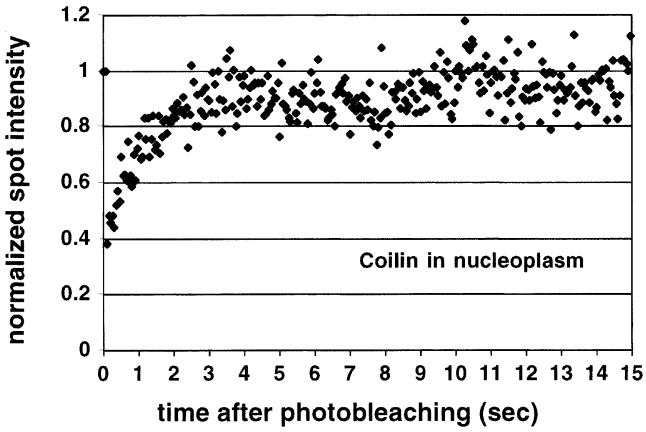

B

molecule	D ± sd ($\mu m^2 sec^{-1}$)	n
Fl-U7	0.26 ± 0.08	19
GFP-coilin	0.40 ± 0.14	20
GFP-TBP	0.33 ± 0.12	26

Figure 5. **FRAP of fluorescein-U7, GFP-coilin, and GFP-TBP in the GV nucleoplasm.** (A) A representative recovery curve of photobleached GFP-coilin in the nucleoplasm of an oil-isolated GV. The curves for fluorescein-U7 and GFP-TBP were similar. (B) Summary of the calculated apparent diffusion coefficient D for fluorescein-U7, GFP-coilin, and GFP-TBP in the nucleoplasm. For each molecule, measurements were made on at least five GVs from at least two animals.

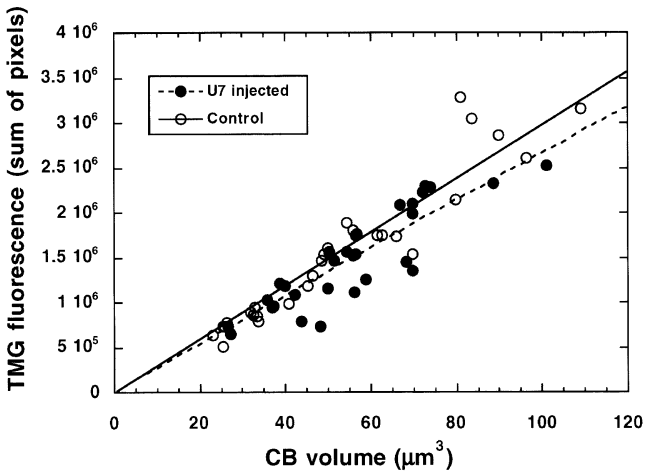

Figure 6. **The concentration of U7 snRNA in CBs is invariant.** CBs in cytological preparations were stained with mAb K121 against the TMG cap found on U7 and other snRNAs. Earlier experiments showed that ~90% of the TMG staining in CBs is due to U7 snRNA. Total fluorescence of individual CBs from control oocytes was then plotted against their volumes (open circles). The slope of the linear relationship is a measure of TMG concentration. CBs from oocytes that had been injected with U7 snRNA were measured in the same way (filled circles). Despite the consequent increase in nucleoplasmic TMG concentration (see Fig. 7), there was no change in the concentration of TMG in CBs.

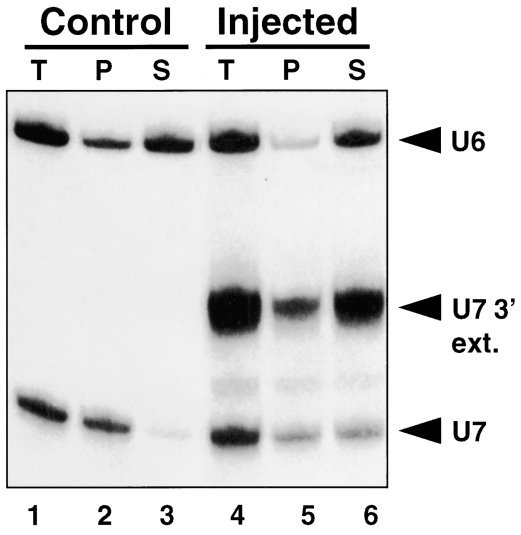

Figure 7. **Exogenous U7 snRNA displaces endogenous U7 from CBs.** Northern blot of RNAs isolated from GVs of control oocytes (lanes 1–3) or oocytes injected with a U7 transcript that contained a 6-nucleotide 3′ extension (lanes 4–6). Lanes 1 and 4 (T) contain the total RNA from two unfractionated GVs. Lanes 2 and 5 (P) are from pellets of two fractionated GVs, and lanes 3 and 6 (S) are the corresponding supernatants. In control GVs, the vast majority of endogenous U7 is in the pellet fraction, presumably in CBs (lane 2). In GVs from injected oocytes, some of the extended U7 occurs in the pellet (lane 5) along with a decreased amount of endogenous U7; the rest of the endogenous U7 in such oocytes now appears in the supernatant (lane 6). U6 snRNA, which is predominantly in the supernatant, serves as a loading control.

U7 snRNA by biochemical fractionation. The goal was to determine if an excess of injected U7 would drive endogenous U7 from the CBs into the nucleoplasm, as had been suggested by earlier cytological experiments (Wu et al., 1996). To differentiate exogenous from endogenous U7, we synthesized a transcript that contained six extra nucleotides at the 3′ end and injected it into the cytoplasm. At various times thereafter, GVs were removed from the oocytes, manually disrupted, and briefly centrifuged. In these preparations, the soluble nucleoplasmic molecules remain in the supernatant fraction, whereas the nuclear organelles (of which only CBs contain U7) sediment as a pellet. The pellet and supernatant fractions were then analyzed by Northern blotting (Fig. 7). The first three lanes show the distribution of U7 in whole GVs, pellet, and supernatant fractions of control GVs. As reported previously (Wu et al., 1996), the nucleoplasm (lane 3) of control GVs is almost devoid of endogenous U7. Lanes 4–6 show the distribution of endogenous and injected U7 in GVs 7 h after injection of the elongated transcript. Endogenous U7 is now distributed roughly equally between the pellet (lane 5) and the supernatant (lane 6). At the same time, some of the injected U7 appears in the pellet (lane 5), presumably because it has entered the CBs. These results demonstrate that endogenous U7 exits the CBs as exogenous U7 enters, suggesting a possible steady-state flux of CB components between the nucleoplasm and CBs.

Steady-state exchange of CB components between the nucleoplasm and CBs

To determine whether CB components exchange between the nucleoplasm and CBs at steady-state, we performed FRAP on U7, GFP-coilin, and GFP-TBP in CBs in oil-isolated GVs. A laser scanning confocal microscope was used to create a diffraction-limited bleach spot inside individual CBs. FRAP of the bleached area was then measured in a single optical plane as a function of time (Fig. 8 A). Results of the FRAP experiments for U7 are summarized in Fig. 8 B. The most obvious feature is the long time for recovery relative to FRAP of the same molecule in the nucleoplasm; minutes rather than seconds. In fact, none of the curves had returned to their full initial value by the time the experiments were terminated at ~0.5 h. Such behavior suggested a multi-phasic recovery, which was confirmed by fitting the curves to a sum of exponentials (supplemental material, available at http://www.jcb.org/cgi/content/full/jcb.200212024/DC1). In each case, there were at least three kinetic components to the recovery. Approximate residence times for these kinetic states were 14 s, 7.2 min, and 33 min for U7 and coilin, and 15 s, 3.3 min, and 34 min for TBP. Controls for spontaneous recovery of fluorescence in CBs were performed on spread preparations that were fixed in 2% PFA. No spontaneous recovery was evident after photobleaching.

The disappearance of the bleach spot within CBs could involve two processes: (1) replacement of photobleached molecules in the CBs with fluorescent molecules from the nucleoplasm; and (2) rearrangement of fluorescent molecules already in the CBs. To assess the relative contributions of these two processes, we photobleached CBs in a band across their middle with the confocal microscope, or in their entirety with a wide-field fluorescence microscope (supple-

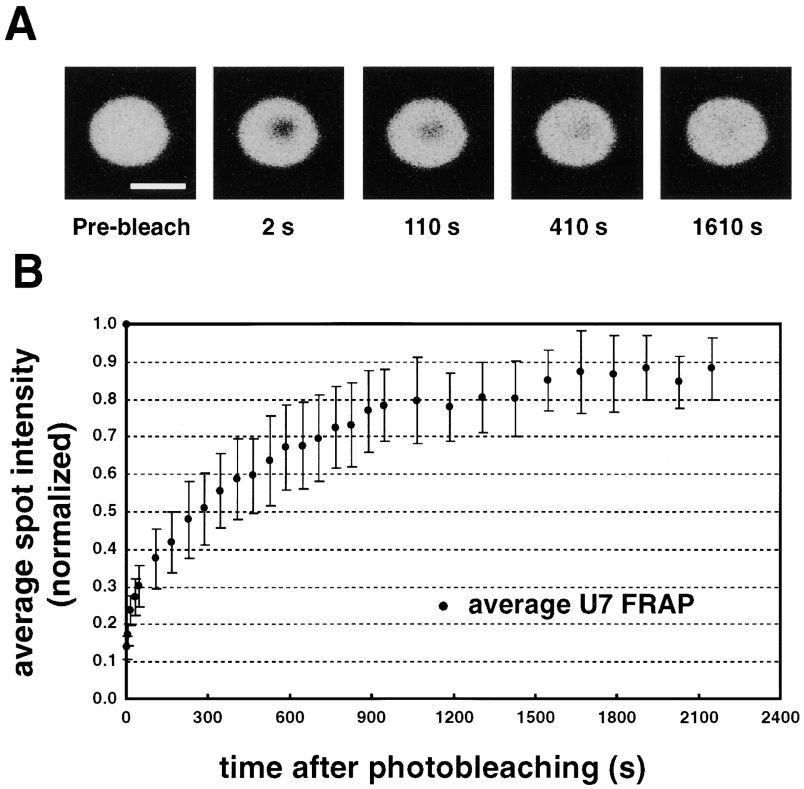

Figure 8. **FRAP of fluorescein-U7 in CBs.** (A) Selected images from a confocal FRAP series of U7 in a single CB. A diffraction-limited spot was bleached inside the CB, and recovery of fluorescence was recorded as a function of time in seconds. Bar, 5 μm. (B) Plot of means and SDs of U7 data from 15 experiments of the sort shown in A. In each experiment, the average intensity of the bleach spot was measured as a function of time. Intensities were normalized to the prebleach value and corrected for minor bleaching during imaging. The curve for GFP-coilin was almost identical to that of U7. For GFP-TBP, the final phase of recovery was somewhat slower.

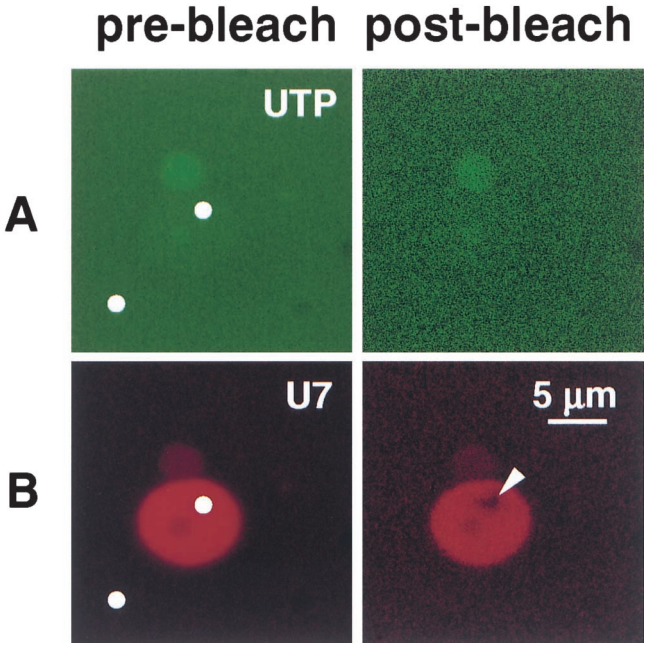

Figure 9. **FRAP of fluorescein-UTP and Alexa 546–U7 in CBs and nucleoplasm.** An oocyte was coinjected in the cytoplasm with fluorescein-UTP and Alexa 546–U7 snRNA. After overnight incubation, the GV was isolated in oil and squashed under a coverslip. Fluorescein-UTP was neither concentrated in nor excluded from CBs relative to the nucleoplasm (A), whereas Alexa 546–U7 accumulated strongly in the same CB (B). Spots were bleached in the nucleoplasm and in the CB (white dots in the prebleach images). Recovery in the fluorescein-UTP channel (A) was too fast to record in both the nucleoplasm and CB after bleaching. Therefore, the postbleach image is uniform in intensity (except for two B-snurposomes; one on the surface and one inside the CB, which bind fluorescein-UTP weakly). Recovery of the bleach spot (arrowhead) inside the CB is very slow in the Alexa 546–U7 channel (B). The postbleach images represent a single confocal scan and are grainier than the prebleach images, which are frame-averaged.

mental material). In both cases, the recovery of fluorescence followed the same kinetics as in the spot-bleach experiments. These experiments indicate that recovery of fluorescence must depend primarily on replacement of photobleached molecules in the CB with fluorescent molecules from the nucleoplasm. Moreover, if fluorescence recovery within the CB were due simply to diffusion, recovery should have been strongly dependent on bleach spot diameter.

The slow fluorescence recovery inside CBs cannot be explained by high CB viscosity

The slow rate at which photobleached U7, coilin, and TBP recovered inside CBs relative to the nucleoplasm is consistent with the idea that these molecules bind transiently to other molecules within CBs. However, it remains a formal possibility that fluorescence recovery within CBs might be impeded by high internal viscosity.

According to the Stokes-Einstein equation, the diffusion coefficient of a molecule is inversely proportional to the viscosity of the medium in which it diffuses. Therefore, other experimental parameters being equal, high internal viscosity could contribute to the slow FRAP inside CBs relative to the nucleoplasm. To address this issue, we performed FRAP on fluorescein-UTP, which is neither excluded from CBs nor concentrated in them relative to the nucleoplasm (Fig. 9 A). The uniform distribution of fluorescein-UTP presumably results from its ability to penetrate CBs without appreciably interacting with CB components. We reasoned that if the inter-

nal milieu of CBs is more viscous than the nucleoplasm, then after photobleaching, fluorescein-UTP within CBs should recover more slowly than fluorescein-UTP in the nucleoplasm.

Oocytes were coinjected into the cytoplasm with fluorescein-UTP and Alexa 546–U7. After overnight incubation, GVs were isolated from the oocytes under oil and gently squashed under a coverslip. In the blue light used for FRAP of fluorescein-UTP (488 nm), CBs fluoresced with the same intensity as the nucleoplasm, and hence, were invisible. Therefore, CBs were located and positioned for FRAP in green light, where they fluoresced bright red because of their high concentration of Alexa 546–U7. FRAP was performed with the same high speed apparatus used for nucleoplasmic diffusion measurements. Fluorescent molecules in an ~1.0-μm spot within a single CB or the nucleoplasm were photobleached by a brief, high intensity pulse of 488-nm laser light, and the subsequent fluorescence recovery was recorded every 50 ms for ~15 s. In each case, complete recovery was achieved by the time the first few data points had been recorded. Although we could not determine accurate diffusion coefficients from these data, it was clear that recovery times were similar in the nucleoplasm and CB, and both were at least three orders of magnitude faster than for U7, coilin, and TBP in CBs. Thus, high internal CB viscosity is unlikely to contribute to the slow FRAP observed for these three CB components.

For purposes of illustration, we performed the same experiment with the confocal microscope. The high intensity pulse of 488-nm light also bleaches Alexa 546–U7, even though 488 nm is well below the absorption peak of the Alexa dye. Recovery of fluorescein-UTP in both the nucleoplasm and the CB occurred before the first postbleach image was taken (Fig. 9 A). Because the recovery of photobleached U7 takes minutes, we could confirm that the CB had been photobleached by observing the red fluorescence of U7 (Fig. 9 B). We could also confirm by focusing that the bleached area lay completely within the CB.

The slow fluorescence recovery inside CBs cannot be explained by high CB density

The diffusion of molecules in subcellular compartments is influenced by additional parameters not considered in the Stokes-Einstein equation (Kao et al., 1993; Seksek et al., 1997). One such parameter is molecular crowding, reflected in the physical density of the compartment under consideration. For example, CBs might consist of a dense meshwork of molecules whose effective pore size limits the free movement of incoming macromolecules. Such a network could, in theory, explain the slow FRAP we observe for fluorescein-U7, GFP-coilin, and GFP-TBP inside CBs. The density of CBs and other nuclear organelles can be estimated by measuring their refractive index with an interferometer microscope (Davies, 1958; Hale, 1958). Such measurements are underway in our laboratory and will be reported in a separate publication. However, simple phase contrast and differential interference contrast observations on oil-isolated nuclei show that CBs are barely visible when surrounded by nucleoplasm, whereas nucleoli and B-snurposomes display higher contrast (Fig. 4, A and B). Because phase contrast and differential interference contrast both depend on differences in refractive index between the specimen and the medium in which it is observed, we can conclude that the refractive index of CBs, and hence their protein concentration, does not differ by more than a few percent from that of the nucleoplasm. A small difference in protein concentration could not account for the >100-fold difference in mobility that we observe for CB components in CBs relative to the same components in the nucleoplasm.

Discussion

High resolution analysis of nuclear structure and function

The emerging field of nuclear dynamics is based heavily on the study of mammalian tissue culture cells. Although such studies provide invaluable information about nuclear structure and function, the somatic nucleus has some inherent disadvantages, chief of which is its small size. Individual intranuclear organelles are correspondingly small, CBs in somatic cells being <1 μm in diameter in most cases. Furthermore, the nucleoplasm of somatic nuclei is not readily distinguishable from other components of the extranucleolar space. These characteristics of somatic nuclei make it difficult to achieve the level of resolution required for a detailed analysis of the steady-state behavior of CB components.

In contrast, a mature oocyte nucleus of *Xenopus* is ~400 μm in diameter. The vast majority of its volume lacks resolvable structure at the light microscope level, and thus can be characterized as nucleoplasm. The remaining volume contains the 18 lampbrush chromosomes plus thousands of nuclear organelles that are readily discernible with transmitted light. A single GV can contain up to 100 CBs with diameters in the range of 2–10 μm. Because of its large size, a GV can be isolated by hand, either in an appropriate saline solution or in oil. Oil-isolated *Xenopus* GVs maintain energy-dependent functions for many hours after removal from the cytoplasm (Lund and Paine, 1990; Paine et al., 1992; Yu et al., 1998). Therefore, this system is useful for studying various aspects of nuclear biochemistry, such as RNA splicing and modification. Here, we have used oil-isolated GVs to follow the in vivo steady-state dynamics of CB components in both CBs and nucleoplasm by FRAP. The same system should be equally valuable for studying other nuclear organelles, such as nucleoli, B-snurposomes, and lampbrush chromosomes.

CB components are freely diffusible in the oocyte nucleoplasm

The translational mobility of a solute in a complex macromolecular mixture is influenced by the fluid-phase viscosity, collision between the solute and macromolecular obstacles, and binding of the solute to other macromolecules (Kao et al., 1993). The contribution of each of these parameters to the mobility of molecules in bulk cytoplasm, cytoplasmic organelles, and membranes has been analyzed extensively because the physical structure of these compartments is thought to impose significant restraint on the rates of biochemical reactions within and between compartments (Kao et al., 1993; Seksek et al., 1997; Dayel et al., 1999). These same parameters undoubtedly influence translational mobility in the nucleus. Here, we have addressed the contribution

of these parameters to the mobility of CB components in CBs and the nucleoplasm.

Recent FRAP measurements on GFP-constructs now suggest that various proteins move freely within the nucleoplasm and also exchange between the nucleoplasm and subnuclear compartments, such as the nucleoli, CBs, and splicing factor compartments (speckles; Misteli et al., 1997; Snaar et al., 2000; Carmo-Fonseca et al., 2002; Chen et al., 2002; Dundr et al., 2002). In the nucleoplasm of mammalian cultured cells, the apparent diffusion coefficient for three GFP-labeled nuclear proteins (HMG-17, SF2/ASF, and fibrillarin) ranged from 0.24 to 0.53 $\mu m^2\ sec^{-1}$ (Phair and Misteli, 2000). Likewise, Politz and colleagues (1999) used a caged fluorescent oligonucleotide hybridized to poly(A) to show that bulk poly(A) RNA had a diffusion coefficient of 0.6 $\mu m^2\ sec^{-1}$ in rat myoblast nuclei. Our values for fluorescein-U7, GFP-coilin, and GFP-TBP in the GV nucleoplasm are similar, 0.26–0.40 $\mu m^2\ sec^{-1}$.

Earlier measurements of FITC-dextran in the nucleoplasm of cultured mammalian cells showed more rapid diffusion with D values ranging from 2.5 to 10 $\mu m^2\ sec^{-1}$ for molecular weights in the range of 70 kD–2 MD (Seksek et al., 1997). It will be interesting to measure FITC-dextran in the GV to determine whether these differences are related to the type of nucleus or to the nature of the molecules.

Reaction limited mobility of CB components in CBs

Fluorescein-U7, GFP-coilin, and GFP-TBP within CBs differ in at least two important respects from the same molecules in the nucleoplasm. First, the steady-state concentration in each case is much higher within the CB than outside. Second, the recovery of fluorescence after bleaching is much slower and shows at least three kinetic components. Slow recovery was also found for GFP-fibrillarin in CBs from human osteosarcoma cells in culture (Snaar et al., 2000), suggesting that CBs in oocytes and somatic tissues may have similar kinetic properties.

CBs and other nuclear organelles lack membranes like those that surround many cytoplasmic organelles or the nucleus itself. Thus, the accumulation of CB components against a concentration gradient is not likely to involve specific pumps or channels like those found in cytoplasmic membranes or the nuclear envelope. In the absence of such mechanisms, specific binding is the most probable factor involved in the accumulation of CB components.

In the simplest binding scenario, components might associate with one or more classes of binding sites within CBs and remain there for a time period well beyond what we have measured experimentally. This type of binding might involve storage of macromolecular complexes to be used days or weeks later by the developing embryo, as is the case of yolk granules in the oocyte cytoplasm. This is clearly not the case for U7 snRNA, coilin, and TBP, where fluorescence recovery occurs on a time scale of minutes. Furthermore, we have shown experimentally that when exogenous U7 is introduced into the GV, endogenous U7 exits the CBs (Fig. 7), whereas the concentration of U7 remains the same (Fig. 6). Thus, U7 in CBs is clearly in equilibrium with U7 in the nucleoplasm on a time scale of minutes, and the same is probably true for coilin and TBP.

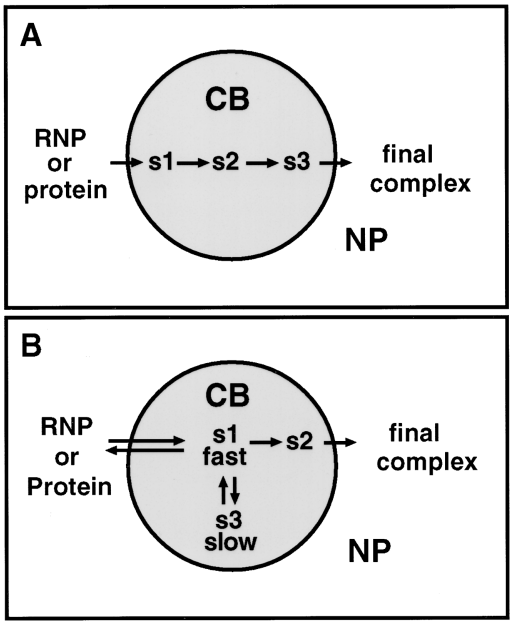

Figure 10. **Kinetic models of CB function.** (A) A sequential model in which molecules pass from one state(s) to the next in a linear, irreversible manner before exiting into the nucleoplasm. This model is incompatible with the kinetics of our FRAP data. (B) A more complex model in which the initial binding event (s1) is reversible and fast, and the slowest step (s3) corresponds to a reservoir that is kinetically isolated from the state that exits the CB (s2). This model is compatible with our FRAP data.

Given that reversible binding best explains the data for U7, coilin, and TBP, we can turn to a more detailed quantitative analysis of the FRAP curves. As discussed in the supplemental material, a good fit of the data for each of these molecules requires at least three exponential terms. That is, the data resolve three states for each protein or RNP within the CB; one that exchanges with $t_{1/2}$ ~15 s, a slower one with $t_{1/2}$ ~3–7 min, and a very slow component with $t_{1/2}$ ~35 min.

We used computer modeling to determine how these three RNP/protein states might be arranged and interconnected in a functional pathway (Phair and Misteli, 2001). A simple hypothesis is that each state represents one stage in the sequential assembly of a macromolecular complex (Fig. 10 A). In any sequential model, the state with the slowest turnover must occupy the largest fraction of the total population of molecules. Our computer analyses indicated that this is not true for any of the three molecules tested in this study. Therefore, we can rule out the linear assembly model for these molecules.

A related but more complex model of assembly can account for our FRAP data (Fig. 10 B). Two features distinguish this model from the linear assembly model. First, movement of molecules between the nucleoplasm and the CB is rapid and reversible. Second, the slow component is removed from the direct assembly pathway, and it exchanges with the first assembly stage. Kinetically, the slow component acts as a reservoir or a slow buffer, but its biological significance remains an open question.

Further biochemical experiments will be required to test the model in Fig. 10 B. However, we feel confident that the

slow compartments exist and are significant features of CB biology. Because enzymes that perform post-transcriptional and post-translational modifications occur in CBs, and because particles comparable in size to ribosomes are present in CBs (Gall et al., 1999), it is tempting to speculate that the slow states we observe in the FRAP experiments represent modification and/or assembly events that occur inside CBs.

Materials and methods

Animals and oocytes

Adult female *Xenopus laevis* (Xenopus1) were anesthetized in 0.1% methanesulfonate salt of 3-aminobenzoic acid ethyl ester (MS222; Sigma-Aldrich) for ~20 min, and a piece of ovary was surgically removed. Unless otherwise stated, oocytes were stored in OR2 saline (Wallace et al., 1973) at 18°C until used.

Plasmids and transcripts

Human TBP cDNA was amplified by PCR from a vector containing the full-length coding sequence with the following primers: upstream, 5′-GCGACGCCGATCGATATGGATCAGAACAACAGCCTGCC-3′; downstream, 5′-GCGACGCCGATCGATGCGTCGTCTTCCTGAATCCC-3′. The underlined sequences are ClaI restriction sites. Amplified products were cloned into the pCRII vector (Invitrogen), grown in Dam$^-$ *Escherichia coli* SCS110, purified by mini-prep (QIAGEN), and then digested with ClaI. The fragment containing the TBP cDNA was gel purified and ligated to ClaI-digested pCS2(GFP) vector (Huang et al., 1999) upstream of the GFP open reading frame. *Xenopus* wild-type U7 snRNA construct no. 401 (Wu et al., 1996) was linearized with SalI and transcribed with T7 polymerase to generate sense-strand molecules for injection. The *Xenopus* GFP-coilin construct (Handwerger et al., 2002) was provided by Z. Wu (Carnegie Institution). Transcripts of fluorescein-U7 snRNA, GFP-coilin mRNA, and GFP-TBP mRNA were synthesized in vitro as described previously (Handwerger et al., 2002).

Microinjections and incubations

Needles were pulled from capillary tubing (0.5-mm inner diameter, 1.2-mm outer diameter) with a vertical pipette puller (David Kopf Instruments). Approximately 1 ng of fluorescein-U7 snRNA, GFP-coilin mRNA, or GFP-TBP mRNA was microinjected in a volume of 9.2–23 nl into the cytoplasm of ~1-mm diam oocytes, using a dissecting microscope in combination with a Nanoject microinjection apparatus (Drummond Scientific). Cells were held for a maximum of 48 h at 18°C in OR2 medium before GV preparations were made.

RNA isolation and Northern blots

GVs were isolated from oocytes and stored for up to 1 h on ice in 100 μl isolation medium (83 mM KCl, 17 mM NaCl, 6.5 mM Na_2HPO_4, 3.5 mM KH_2PO_4, 1 mM $MgCl_2$, and 1 mM dithiothreitol, pH 7.0). RNA was extracted and precipitated as described previously (Gall et al., 1999). Samples were electrophoresed on a 12% polyacrylamide/8M urea/TBE gel at 35 mA for 1.5 h. Northern blots and UV cross-linking were performed as described previously (Bellini and Gall, 1998) with probes of antisense U7 snRNA (10^6 cpm/ml; Wu and Gall, 1993) and U6 snRNA (2.5×10^3 cpm/ml; Wu et al., 1991). Blots were exposed to a PhosphorImager screen, and the resultant images were scanned with a Storm 860 detector and software (Molecular Dynamics, Inc.).

Protein isolation, protein gels, immunoprecipitation, and Western blots

GVs were isolated from oocytes and stored for up to 1 h on ice in isolation medium. GVs were mixed with an equal volume of 2× gel buffer (Laemmli, 1970) and loaded onto a 10% SDS-PAGE mini-gel (Bio-Rad Laboratories). Gels were run for 1 h at 30 mA and blotted onto Immobilon-P nylon filter (Millipore) at 50 V for 4 h at 4°C. Blots were briefly immersed in methanol, rinsed in transfer buffer, and blocked overnight at 4°C in 5% nonfat dry milk in PBS. Membranes were washed three times for a total of 30 min in 0.05% Tween 20 in PBS and incubated for 1 h at RT in primary antibody. Blots were washed and incubated as above with secondary antibody that was either alkaline phosphatase–linked goat anti–rabbit IgG (1:1,000) in 0.025% Tween 20 in PBS, or goat anti–mouse IgG (1:10,000; Amersham Biosciences). After washing, the membrane was exposed to developer according to the manufacturer's protocol (ECF kit; Amersham Biosciences). An image of the chemifluorescence was obtained with the Storm 860 detector and software (Molecular Dynamics, Inc.).

Immunofluorescence and quantitation

Nuclear spreads were prepared as described previously (Gall et al., 1999). The resulting slides were blocked for 10 min in PBS containing 0.2% cold water fish gelatin (Sigma-Aldrich), 5% BSA, and 0.02% sodium azide. GV spreads were incubated with 10 μl of 1 μg/ml mAb K121 (Oncogene Research Products) for 1 h at RT. Slides were washed 3–5 min with PBS and incubated for 1 h with 10 μl of 1 μg/ml Alexa 488–labeled goat anti–mouse IgG (Molecular Probes, Inc.). The slides were again washed with PBS and mounted in 50% glycerol containing 1 mg/ml 1,4-diaminobenzene to retard fading. Images of fluorescent CBs were captured on a CCD camera (MicroMax; Princeton Instruments) and stored as IP Lab Spectrum files (Scanalytics) or as TIFF files in Adobe Photoshop®. mAb Y12 was provided by J. Steitz (Yale University, New Haven, CT), and mAb H1 was provided by R. Tuma and M. Roth (Fred Hutchinson Cancer Research Center, Seattle, WA).

Preparation of oil-isolated GVs

Single oocytes that had been injected with fluorescein-U7, GFP-coilin mRNA, or GFP-TBP mRNA were transferred from OR2 saline to a piece of Whatman #1 filter paper (Whatman, Ltd.). Most of the aqueous medium surrounding each oocyte was absorbed by the filter paper. The oocyte was then transferred to a 35-mm Petri dish containing mineral oil (EC No. 232–455–8; Sigma-Aldrich) and the GV was removed manually with jeweler's forceps (Lund and Paine, 1990; Paine et al., 1992). Individual GVs were transferred to a standard 3″ × 1″ microscope slide in 5 μl of oil and were gently squashed under a 22-mm^2 glass coverslip. After the oil had spread to the edges of the coverslip by capillary action, the sample was observed in the microscope.

FRAP of CBs

For confocal FRAP, oil-isolated GVs were prepared as above. Imaging and bleaching were conducted on a laser scanning confocal microscope (TCS SF2; Leica) using a 100×, NA 1.4 oil immersion objective. Pre- and post-bleach images were collected with the 488-nm line of an argon laser set at minimal output. Each consisted of a single optical section through the center of a CB (512 × 512 pixels; 2× frame-averaged; 25% gain of the acousto-optical tunable filter). A diffraction-limited spot was photobleached inside the CBs by applying full intensity of the beam for 500 ms without scanning. After bleaching, images were scanned every 15 s for 45 s, then every minute until there was no visible difference in fluorescence between the bleached and nonbleached areas (typically 20–30 min). The average pixel intensity within bleached and unbleached areas was quantified with MetaMorph® software (Universal Imaging Corp.). All bleach spot values were corrected for the amount of bleaching that occurred during image acquisition and were then normalized to the prebleach value.

FRAP measurements in the nucleoplasm

Oil-isolated GVs from injected oocytes were prepared for microscopy as above. A fluorescence microscope (Axioplan; Carl Zeiss MicroImaging, Inc.) fitted with a Plan-Neofluar objective (100× oil, NA 1.30) was used to select an area of the GV that was devoid of nucleoli, B-snurposomes, and CBs. An attenuated beam from a 488-nm argon laser was focused on an ~1.0-μm spot of nucleoplasm, and the baseline fluorescence intensity was measured with a photomultiplier tube. The sample was then bleached with full laser intensity for 20 ms. Recovery of fluorescence was recorded every 50 ms with the attenuated beam over a period of 15–20 s and analyzed with custom software (M. Edidin, Johns Hopkins University, Baltimore, MD). To display the recovery series, raw data points were exported to Microsoft Excel software.

Online supplemental material

The online supplemental material gives details on the compartment models and on fitting the FRAP curves to a sum of exponentials. The procedure for wide-field FRAP is also given. Online supplemental material available at http://www.jcb.org/cgi/content/full/jcb.200212024/DC1.

We thank the following for valuable technical assistance and discussions of this work: M. Edidin, Q. Tang, D. Barrick, R. Cone, and D. Wirtz. Analysis of the FRAP data was conducted in collaboration with R. Phair (BioInformatics Services, Rockville, MD).

This work was supported in part by Research Grant GM33397 from the National Institute of General Medical Sciences of the National Institutes of Health (to J.G. Gall). J.G. Gall is American Cancer Society Professor of Developmental Genetics.

Submitted: 3 December 2002
Revised: 7 January 2003
Accepted: 8 January 2003

References

Andrade, L.E.C., E.K.L. Chan, I. Raška, C.L. Peebles, G. Roos, and E.M. Tan. 1991. Human autoantibody to a novel protein of the nuclear coiled body: immunological characterization and cDNA cloning of p80-coilin. *J. Exp. Med.* 173:1407–1419.

Axelrod, D., D.E. Koppel, J. Schlessinger, E. Elson, and W.W. Webb. 1976. Mobility measurement by analysis of fluorescence photobleaching recovery kinetics. *Biophys. J.* 16:1055–1069.

Bauer, D.W., and J.G. Gall. 1997. Coiled bodies without coilin. *Mol. Biol. Cell.* 8:73–82.

Bellini, M., and J.G. Gall. 1998. Coilin can form a complex with the U7 small nuclear ribonucleoproteins particles. *Mol. Biol. Cell.* 9:2987–3001.

Birnstiel, M.L., and F.J. Schaufele. 1988. Structure and function of minor snRNPs. *In* Structure and Function of Major and Minor Small Nuclear Ribonucleoproteins. M.L. Birnstiel, editor. Springer-Verlag, Berlin. 155–182.

Brahms, H., L. Meheus, V. de Brabandere, U. Fischer, and R. Lührmann. 2001. Symmetrical dimethylation of arginine residues in spliceosomal Sm protein B/B' and the Sm-like protein LSm4, and their interaction with the SMN protein. *RNA.* 7:1531–1542.

Cajal, S.R.y. 1903. Un sencillo metodo de coloracion seletiva del reticulo protoplasmatico y sus efectos en los diversos organos nerviosos de vertebrados e invertebrados. *Trab. Lab. Invest. Biol.* 2:129–221.

Carmo-Fonseca, M., M. Platani, and J.R. Swedlow. 2002. Macromolecular mobility inside the cell nucleus. *Trends Cell Biol.* 12:491–495.

Chen, D., C.S. Hinkley, R.W. Henry, and S. Huang. 2002. TBP dynamics in living human cells: constitutive association of TBP with mitotic chromosomes. *Mol. Biol. Cell.* 13:276–284.

Davies, H.G. 1958. The determination of mass and concentration by microscope interferometry. *In* General Cytochemical Methods. J.F. Danielli, editor. Academic Press, New York. 55–161.

Dayel, M.J., E.F.Y. Hom, and A.S. Verkman. 1999. Diffusion of green fluorescent protein in the aqueous-phase lumen of endoplasmic reticulum. *Biophys. J.* 76:2843–2851.

Dewey, T.G. 1991. Biophysical and Biochemical Aspects of Fluorescence Spectroscopy. Plenum Press, New York. 294 pp.

Dundr, M., U. Hoffmann-Rohrer, Q. Hu, I. Grummt, L.I. Rothblum, R.D. Phair, and T. Misteli. 2002. A kinetic framework for a mammalian RNA polymerase in vivo. *Science.* 298:1623–1626.

Gall, J.G. 2000. Cajal bodies: the first 100 years. *Annu. Rev. Cell Dev. Biol.* 16: 273–300.

Gall, J.G., M. Bellini, Z. Wu, and C. Murphy. 1999. Assembly of the nuclear transcription and processing machinery: Cajal bodies (coiled bodies) and transcriptosomes. *Mol. Biol. Cell.* 10:4385–4402.

Hale, A.J. 1958. The interference microscope in biological research. E. and S. Livingstone, Edinburgh. 114 pp.

Handwerger, K.E., Z. Wu, C. Murphy, and J.G. Gall. 2002. Heat shock induces mini-Cajal bodies in the *Xenopus* germinal vesicle. *J. Cell Sci.* 115:2011–2020.

Hebert, M.D., P.W. Szymczyk, K.B. Shpargel, and A.G. Matera. 2001. Coilin forms the bridge between Cajal bodies and SMN, the spinal muscular atrophy protein. *Genes Dev.* 15:2720–2729.

Hebert, M.D., R. Pillai, K.B. Shpargel, J.K. Ospina, D. Schümperli, and A.G. Matera. 2002. Coilin methylation regulates nuclear body formation. *Dev. Cell.* 3:329–337.

Huang, H., N. Marsh-Armstrong, and D.D. Brown. 1999. Metamorphosis is inhibited in transgenic *Xenopus laevis* tadpoles that overexpress type III deiodinase. *Proc. Natl. Acad. Sci. USA.* 96:962–967.

Kao, H.P., J.R. Abney, and A.S. Verkman. 1993. Determinants of the translational mobility of a small solute in cell cytoplasm. *J. Cell Biol.* 120:175–184.

Laemmli, U.K. 1970. Cleavage of structural proteins during the assembly of the head of bacteriophage T4. *Nature.* 227:680–685.

Lund, E., and P. Paine. 1990. Nonaqueous isolation of transcriptionally active nuclei from *Xenopus* oocytes. *Methods Enzymol.* 181:36–43.

Matera, A.G. 1999. Nuclear bodies: multifaceted subdomains of the interchromatin space. *Trends Cell Biol.* 9:302–309.

Mattaj, I.W. 1988. UsnRNP assembly and transport. *In* Structure and Function of Major and Minor Small Nuclear Ribonucleoprotein Particles. M.L. Birnstiel, editor. Springer-Verlag, Berlin. 100–114.

Misteli, T., J.F. Cáceres, and D.L. Spector. 1997. The dynamics of a pre-mRNA splicing factor in living cells. *Nature.* 387:523–527.

Narayanan, A., W. Speckmann, R. Terns, and M.P. Terns. 1999. Role of the box C/D motif in localization of small nucleolar RNAs to coiled bodies and nucleoli. *Mol. Biol. Cell.* 10:2131–2147.

Paine, P.L., M.E. Johnson, Y.-T. Lau, L.J.M. Tluczek, and D.S. Miller. 1992. The oocyte nucleus isolated in oil retains in vivo structure and functions. *Biotechniques.* 13:238–245.

Phair, R.D., and T. Misteli. 2000. High mobility of proteins in the mammalian cell nucleus. *Nature.* 404:604–609.

Phair, R.D., and T. Misteli. 2001. Kinetic modelling approaches to in vivo imaging. *Nat. Rev. Mol. Cell Biol.* 2:898–907.

Pillai, R.S., C.L. Will, R. Lührmann, D. Schümperli, and B. Müller. 2001. Purified U7 snRNPs lack the Sm proteins D1 and D2 but contain Lsm10, a new 14 kDa Sm D1-like protein. *EMBO J.* 20:5470–5479.

Politz, J.C., R.A. Tuft, T. Pederson, and R.H. Singer. 1999. Movement of nuclear poly(A) RNA throughout the interchromatin space in living cells. *Curr. Biol.* 9:285–291.

Raška, I., L.E.C. Andrade, R.L. Ochs, E.K.L. Chan, C.-M. Chang, G. Roos, and E.M. Tan. 1991. Immunological and ultrastructural studies of the nuclear coiled body with autoimmune antibodies. *Exp. Cell Res.* 195:27–37.

Seksek, O., J. Biwersi, and A.S. Verkman. 1997. Translational diffusion of macromolecule-sized solutes in cytoplasm and nucleus. *J. Cell Biol.* 138:131–142.

Sleeman, J.E., and A.I. Lamond. 1999. Newly assembled snRNPs associate with coiled bodies before speckles, suggesting a nuclear snRNP maturation pathway. *Curr. Biol.* 9:1065–1074.

Sleeman, J., C.E. Lyon, M. Platani, J.-P. Kreivi, and A.I. Lamond. 1998. Dynamic interactions between splicing snRNPs, coiled bodies and nucleoli revealed using snRNP protein fusions to the green fluorescent protein. *Exp. Cell Res.* 243:290–304.

Smith, H.O., K. Tabiti, G. Schaffner, D. Soldati, U. Albrecht, and M.L. Birnstiel. 1991. Two-step affinity purification of U7 small nuclear ribonucleoprotein particles using complementary biotinylated 2′-O-methyl oligoribonucleotides. *Proc. Natl. Acad. Sci. USA.* 88:9784–9788.

Snaar, S., K. Wiesmeijer, A. Jochemsen, H. Tanke, and R. Dirks. 2000. Mutational analysis of fibrillarin and its mobility in living human cells. *J. Cell Biol.* 151:653–662.

Tucker, K.E., M.T. Berciano, E.Y. Jacobs, D.F. LePage, K.B. Shpargel, J.J. Rossire, E.K.L. Chan, M. Lafarga, R.A. Conlon, and A.G. Matera. 2001. Residual Cajal bodies in coilin knockout mice fail to recruit Sm snRNPs and SMN, the spinal muscular atrophy gene product. *J. Cell Biol.* 154:293–307.

Verheggen, C., J. Mouaikel, M. Thiry, J.-M. Blanchard, D. Tollervey, R. Bordonné, D.L.J. Lafontaine, and E. Bertrand. 2001. Box C/D small nucleolar RNA trafficking involves small nucleolar RNP proteins, nucleolar factors and a novel nuclear domain. *EMBO J.* 20:5480–5490.

Verheggen, C., D.L.J. Lafontaine, D. Samarsky, J. Mouaikel, J.-M. Blanchard, R. Bordonné, and E. Bertrand. 2002. Mammalian and yeast U3 snoRNPs are matured in specific and related nuclear compartments. *EMBO J.* 21:2736–2745.

Wallace, R.A., D.W. Jared, J.N. Dumont, and M.W. Sega. 1973. Protein incorporation by isolated amphibian oocytes. 3. Optimum incubation conditions. *J. Exp. Zool.* 184:321–333.

Wu, C.-H.H., and J.G. Gall. 1993. U7 small nuclear RNA in C snurposomes of the *Xenopus* germinal vesicle. *Proc. Natl. Acad. Sci. USA.* 90:6257–6259.

Wu, C.-H.H., C. Murphy, and J.G. Gall. 1996. The Sm binding site targets U7 snRNA to coiled bodies (spheres) of amphibian oocytes. *RNA.* 2:811–823.

Wu, Z., C. Murphy, H.G. Callan, and J.G. Gall. 1991. Small nuclear ribonucleoproteins and heterogeneous nuclear ribonucleoproteins in the amphibian germinal vesicle: loops, spheres, and snurposomes. *J. Cell Biol.* 113:465–483.

Wu, Z., C. Murphy, and J.G. Gall. 1994. Human p80-coilin is targeted to sphere organelles in the amphibian germinal vesicle. *Mol. Biol. Cell.* 5:1119–1127.

Yu, Y.-T., M.-D. Shu, and J. Steitz. 1998. Modifications of U2 snRNA are required for snRNP assembly and pre-mRNA splicing. *EMBO J.* 17:5783–5795.